

# Sensing Matrix Optimization for Block-Sparse Decoding

Lihi Zelnik-Manor, *Member, IEEE*, Kevin Rosenblum, and Yonina C. Eldar, *Senior Member, IEEE*

**Abstract**—Recent work has demonstrated that using a carefully designed sensing matrix rather than a random one, can improve the performance of compressed sensing. In particular, a well-designed sensing matrix can reduce the coherence between the atoms of the equivalent dictionary, and as a consequence, reduce the reconstruction error. In some applications, the signals of interest can be well approximated by a union of a small number of subspaces (e.g., face recognition and motion segmentation). This implies the existence of a dictionary which leads to *block-sparse* representations. In this work, we propose a framework for sensing matrix design that improves the ability of block-sparse approximation techniques to reconstruct and classify signals. This method is based on minimizing a weighted sum of the interblock coherence and the subblock coherence of the equivalent dictionary. Our experiments show that the proposed algorithm significantly improves signal recovery and classification ability of the *Block-OMP* algorithm compared to sensing matrix optimization methods that do not employ block structure.

**Index Terms**—Block-sparsity, compressed sensing, sensing matrix design.

## I. INTRODUCTION

THE framework of compressed sensing aims at recovering an unknown vector  $x \in R^N$  from an underdetermined system of linear equations  $y = Ax$ , where  $A \in R^{M \times N}$  is a sensing matrix, and  $y \in R^M$  is an observation vector with  $M < N$ . Since the system is under-determined,  $x$  can not be recovered without additional information. In [1] and [2], it was shown that when  $x$  is known to have a sufficiently sparse representation, and when  $A$  is randomly generated,  $x$  can be recovered uniquely with high probability from the measurements  $y$ . More specifically, the assumption is that  $x$  can be represented as  $x = D\theta$  for some orthogonal dictionary  $D \in R^{N \times N}$ , where  $\theta \in R^N$  is sufficiently sparse. The vector  $x$  can then be recovered regardless of  $D$  and irrespective of the locations of the nonzero entries of  $\theta$ . This can be achieved by approximating the sparsest representation  $\theta$  using methods such as *Basis Pursuit*

(BP) [3] and *Orthogonal Matching Pursuit* (OMP) [4], [5]. In practice, overcomplete dictionaries  $D \in R^{N \times K}$  with  $K \geq N$  lead to improved sparse representations and are better suited for most applications. Therefore, we treat the more general case of overcomplete dictionaries in this paper.

A simple way to characterize the recovery ability of sparse approximation algorithms was presented in [4], using the coherence between the columns of the equivalent dictionary  $E = AD$ . When the coherence is sufficiently low, OMP and BP are guaranteed to recover the sparse vector  $\theta$ . Accordingly, recent work [6]–[8] has demonstrated that designing a sensing matrix such that the coherence of  $E$  is low improves the ability to recover  $\theta$ . The proposed methods yield good results for general sparse vectors.

In some applications, however, the representations have a unique sparsity structure that can be exploited. Our interest is in the case of signals that are drawn from a union of a small number of subspaces [9]–[11]. This occurs naturally, for example, in face recognition [12], [13], motion segmentation [14], multiband signals [15]–[17], measurements of gene expression levels [18], and more. For such signals, sorting the dictionary atoms according to the underlying subspaces leads to sparse representations which exhibit a block-sparse structure, i.e., the nonzero coefficients in  $\theta$  occur in clusters of varying sizes. Several methods, such as *Block-BP* (BBP) [11], [19], [20], also referred to as Group lasso [21]–[23], and *Block-OMP* (BOMP) [24], [25] have been proposed to take advantage of this block structure in recovering the block-sparse representations  $\theta$ . Bounds on the recovery performance were presented in [11] based on the block restricted isometry property (RIP), and in [24] using appropriate coherence measures. In particular, it was shown in [24] that under conditions on the *interblock coherence* (i.e., the maximal coherence between two blocks) and the *subblock coherence* (i.e., the maximal coherence between two atoms in the same block) of the equivalent dictionary  $E$ , Block-OMP is guaranteed to recover the block-sparse vector  $\theta$ .

In this paper we propose a method for designing a sensing matrix, assuming that a block-sparsifying dictionary is provided. Our approach improves the recovery ability of block-sparse approximation algorithms by targeting the Gram matrix of the equivalent dictionary, an approach similar in spirit to that of [7], [8]. While [7] and [8] targeted minimization of the coherence between atoms, our method, which will be referred to as *Weighted Coherence Minimization* (WCM), aims at reducing a weighted sum of the interblock coherence and the subblock coherence.

It turns out that the weighted coherence objective is hard to minimize directly. To derive an efficient algorithm, we use the bound-optimization method, and replace our objective with an

Manuscript received September 17, 2010; revised February 03, 2011; accepted May 23, 2011. Date of publication June 09, 2011; date of current version August 10, 2011. The associate editor coordinating the review of this manuscript and approving it for publication was Prof. Sofia C. Olhede. The work of L. Zelnik-Manor was supported by Marie Curie IRG-208529 and by the Ollendorf foundation. The work of Y. Eldar was supported in part by a Magnetron grant from the Israel Ministry of Industry and Trade and by the Israel Science Foundation by Grant 170/10.

The authors are with the Department of Electrical Engineering, Technion—Israel Institute of Technology, Haifa, Israel (e-mail: lihi@ee.technion.ac.il; kevin@tx.technion.ac.il; yonina@ee.technion.ac.il).

Color versions of one or more of the figures in this paper are available online at <http://ieeexplore.ieee.org>.

Digital Object Identifier 10.1109/TSP.2011.2159211

easier to minimize surrogate function that is updated in each optimization step [26]. We develop a closed form solution for minimizing the surrogate function in each step, and prove that its iterative minimization is guaranteed to converge to a local solution of the original problem.

Our experiments reveal that minimizing the subblock coherence is more important than minimizing the interblock coherence. By giving more weight to minimizing the subblock coherence, the proposed algorithm yields sensing matrices that lead to equivalent dictionaries with nearly orthonormal blocks. Simulations show that such sensing matrices significantly improve signal reconstruction and signal classification results compared to previous approaches that do not employ block structure.

We begin by reviewing previous work on sensing matrix design in Section II. In Section III we introduce our definitions of total interblock coherence and total subblock coherence. We then present the objective for sensing matrix design, and show that it can be considered as a direct extension of the one used in [8] to the case of blocks. We present the WCM algorithm for minimizing the proposed objective in Section IV and prove its convergence in Appendix A. We evaluate the performance of the proposed algorithm and compare it to previous work in Section V.

Throughout the paper, we denote vectors by lowercase letters, e.g.,  $x$ , and matrices by uppercase letters, e.g.,  $A$ .  $A'$  is the transpose of  $A$ . The  $j$ th column of the matrix  $A$  is  $A_j$ , and the  $i$ th row is  $A^i$ . The entry of  $A$  in the row with index  $i$  and the column with index  $j$  is  $A_j^i$ . We define the Frobenius norm by  $\|A\|_F \equiv \sqrt{\sum_j \|A_j\|_2^2}$ , and the  $l_p$ -norm of a vector  $x$  by  $\|x\|_p$ . The  $l_0$ -norm  $\|x\|_0$  counts the number of non-zero entries in  $x$ . We denote the identity matrix by  $I$  or  $I_s$  when the dimension is not clear from the context. The spectral norm of  $B$  is the square root of the largest eigenvalue  $\lambda_{\max}(B'B)$  of the positive-semidefinite matrix  $B'B$ .

## II. PRIOR WORK ON SENSING MATRIX DESIGN

The goal of sensing matrix design is to construct a sensing matrix  $A \in R^{M \times N}$  with  $M < N$  that improves the recovery ability for a given sparsifying dictionary  $D \in R^{N \times K}$  with  $K \geq N$ . In other words,  $A$  is designed to improve the ability of sparse approximation algorithms such as BP and OMP to recover the sparsest representation  $\theta$  from

$$y = AD\theta = E\theta \quad (1)$$

where  $E$  is the equivalent dictionary. In this section we briefly review the sensing matrix design method introduced by Duarte-Carvajalino and Sapiro [8]. Their algorithm was shown to provide significant improvement in reconstruction success.

The motivation to design sensing matrices stems from the theoretical work of [4], where it was shown that BP and OMP succeed in recovering  $\theta$  when the following condition holds:

$$\|\theta\|_0 \leq \frac{1}{2} \left( 1 + \frac{1}{\mu} \right). \quad (2)$$

Here  $\mu$  is the coherence defined by

$$\mu \equiv \max_{i \neq j} \frac{|E_i' E_j|}{\|E_i\|_2 \|E_j\|_2}. \quad (3)$$

The smaller  $\mu$ , the higher the bound on the sparsity of  $\theta$ . Since  $E$  is overcomplete, and as a consequence not orthogonal,  $\mu$  will always be strictly positive. Condition (2) is a worst-case bound and does not reflect the average recovery ability of sparse approximation methods. However, it does suggest that recovery may be improved when  $E$  is as orthogonal as possible.

Motivated by these observations, Duarte-Carvajalino and Sapiro [8] proposed designing a sensing matrix  $A$  by minimizing  $\|E'E - I\|_F^2$ . This problem can be written as

$$\min_A \|E'E - I\|_F^2 = \min_A \|D'A'AD - I\|_F^2. \quad (4)$$

It is important to note that rather than minimizing  $\mu$ , (4) minimizes the sum of the squared inner products of all pairs of atoms in  $E$ , referred to as the total coherence  $\mu^t$

$$\mu^t = \sum_{j, i \neq j} (E_i' E_j)^2. \quad (5)$$

At the same time, solving (4) keeps the norms of the atoms close to 1.

While an approximate solution to (4) has already been presented in [8], we provide an exact solution that will be of use in the next sections. To solve (4), we rewrite its objective using the well-known relation between the Frobenius norm and the trace,  $\|C\|_F^2 = \text{tr}(CC')$

$$\begin{aligned} \|E'E - I_K\|_F^2 &= \text{tr}(E'EE'E - 2E'E + I_K) \\ &= \text{tr}(EE'EE' - 2EE' + I_M) \\ &\quad + (K - M) \\ &= \|EE' - I_M\|_F^2 + (K - M) \\ &= \|ADD'A' - I_M\|_F^2 + (K - M). \end{aligned} \quad (6)$$

Since the first term in (6) is always positive, the objective of (4) is lower bounded by  $\|E'E - I\|_F^2 \geq K - M$ .

From (6) it follows that minimizing (4) is equivalent to the minimization of  $\|ADD'A' - I_M\|_F^2$ . A solution to this problem can be achieved in closed form as follows. Let  $U\Lambda U'$  be the eigenvalue decomposition of  $DD'$ , and let  $\Gamma_{M \times N} = AU\Lambda^{\frac{1}{2}}$ . Then, (4) is equivalent to

$$\min_A \|\Gamma\Gamma' - I\|_F^2. \quad (7)$$

This problem is solved by choosing  $\Gamma$  to be any matrix with orthonormal rows, such as  $\Gamma = [I_M \ 0]$ , leading to  $\Gamma\Gamma' = I$ . The optimal sensing matrix is then given by  $A = \Gamma\Lambda^{-\frac{1}{2}}U'$ . Here, and throughout the paper, we assume that  $D$  has full row rank, guaranteeing that  $\Lambda$  is invertible. Note that the global minimum of the objective in (4) equals  $K - M$ . The benefits of using such a sensing matrix were shown empirically in [8].

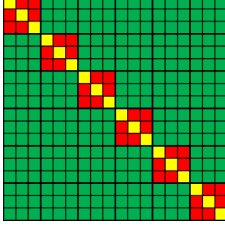


Fig. 1. A graphical depiction of the Gram matrix  $G$  of an equivalent dictionary  $E$  with 6 blocks of size 3. The entries belonging to different blocks are in green, the off-diagonal entries belonging to the same block are in red, and the diagonal entries are in yellow.

### III. SENSING MATRIX DESIGN FOR BLOCK-SPARSE DECODING

The design of a sensing matrix according to [8] does not take advantage of block structure in the sparse representations of the data. In this section we formulate the problem of sensing matrix design for block-sparse decoding. We first introduce the basic concepts of block-sparsity, and then present an objective which can be seen as an extension of (4) to the case of block-sparsity.

#### A. Block-Sparse Decoding

The framework of block-sparse decoding aims at recovering an unknown vector  $x \in R^N$  from an under-determined system of linear equations  $y = Ax$ , where  $A \in R^{M \times N}$  is a sensing matrix, and  $y \in R^M$  is an observation vector with  $M < N$ . The difference with sparse recovery lies in the assumption that  $x$  has a sufficiently block-sparse representation  $\theta \in R^N$  with respect to some block-sparsifying dictionary  $D \in R^{N \times N}$ . The vector  $x$  can then be recovered by approximating the block-sparsest representation corresponding to the measurements  $y$  using methods such as Block-BP (BBP) [11], [19], [20] and Block-OMP (BOMP) [24], [25].

A block-sparsifying dictionary  $D$  is a dictionary whose atoms are sorted in blocks which enable block-sparse representations for a set of signals. We can represent  $D$  as a concatenation of  $B$  column-blocks  $D[j]$  of size  $N \times s_j$ , where  $s_j$  is the number of atoms belonging to the  $j$ th block

$$D = [D[1] D[2] \dots D[B]].$$

Similarly, we view the representation  $\theta$  as a concatenation of  $B$  blocks  $\theta[j]$  of length  $s_j$

$$\theta = [\theta[1] \theta[2] \dots \theta[B]]'.$$

We say that a representation  $\theta$  is  $k$ -block-sparse if its nonzero values are concentrated in  $k$  blocks only. This is denoted by  $\|\theta\|_{2,0} \leq k$ , where

$$\|\theta\|_{2,0} = \sum_{j=1}^B I(\|\theta[j]\|_2 > 0).$$

The indicator function  $I(\cdot)$  counts the number of blocks in  $\theta$  with nonzero Euclidean norm.

#### B. Problem Definition

For a given block-sparsifying dictionary  $D \in R^{N \times K}$  with  $K \geq N$ , we wish to design a sensing matrix  $A \in R^{M \times N}$  that

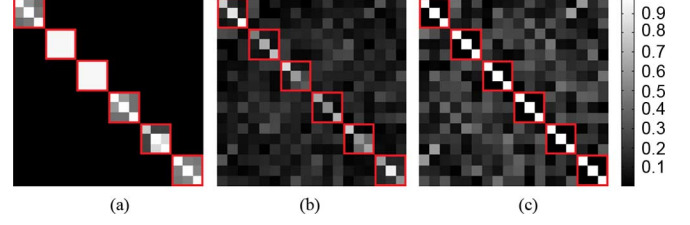


Fig. 2. Examples of the absolute value of the Gram matrix of an equivalent dictionary for  $\alpha = 0.01$  (a)  $\alpha = 0.5$  (b), and  $\alpha = 0.99$  (c) where the sensing matrix of size  $12 \times 18$  was found by solving (13) given a randomly selected square dictionary composed of 6 blocks of size 3. The subblock entries are highlighted by red squares.

improves the recovery ability of block-sparse approximation algorithms. Note that we allow  $D$  to be overcomplete. A performance bound on the recovery success of block-sparse signals has been developed in [24] for the case of a dictionary  $D$  with blocks of a fixed size  $s$  (i.e.,  $s_i = s_j = s$ ) and an equivalent dictionary  $E = AD$  with normalized columns. The bound is a function of the Gram matrix  $G \in R^{K \times K}$  of the equivalent dictionary, defined as  $E'E$ . The  $(i, j)$ th block of  $G$ ,  $E[i]'E[j]$ , is denoted by  $G[i, j] \in R^{s_i \times s_j}$ . The  $(i, j)$ th block of any other  $K \times K$  matrix will be denoted similarly. It was shown in [24] that BBP and BOMP succeed in recovering the block sparsest representation  $\theta$  corresponding to the measurements  $y = E\theta$  when the following condition holds:

$$\|\theta\|_{2,0} < \frac{1}{2s} \left( \mu_B^{-1} + s - (s-1) \frac{\nu}{\mu_B} \right). \quad (8)$$

Here

$$\mu_B \equiv \max_{j, i \neq j} \frac{1}{s} \sqrt{\lambda_{\max}(G[i, j]'G[i, j])}$$

is the *interblock coherence* and

$$\nu \equiv \max_j \max_{n, m \neq n} |(G[j, j])_n^m|$$

is the *subblock coherence*. The interblock coherence  $\mu_B$  is a generalization of the coherence  $\mu$ , and describes the global properties of the equivalent dictionary. More specifically,  $\mu_B$  measures the cosine of the minimal angle between two blocks in  $E$ . The subblock coherence  $\nu$  describes the local properties of the dictionary, by measuring the cosine of the minimal angle between two atoms in the same block in  $E$ . Note, that when  $s = 1$ , (8) reduces to the bound in the sparse case (2). The term  $\mu_B^{-1}$  in (8) suggests that  $\mu_B$  needs to be reduced in order to loosen the bound. On the other hand, the term  $-(s-1) \frac{\nu}{\mu_B}$  implies that the ratio  $\frac{\nu}{\mu_B}$  should be small. This leads to a tradeoff between minimizing  $\mu_B$  and minimizing  $\nu$  to loosen the bound, which is reflected in the sensing matrix design objective presented later in this section.

Condition (8) is a worst case bound and does not represent the average recovery ability of block-sparse approximation methods. It does suggest, however, that in order to improve the

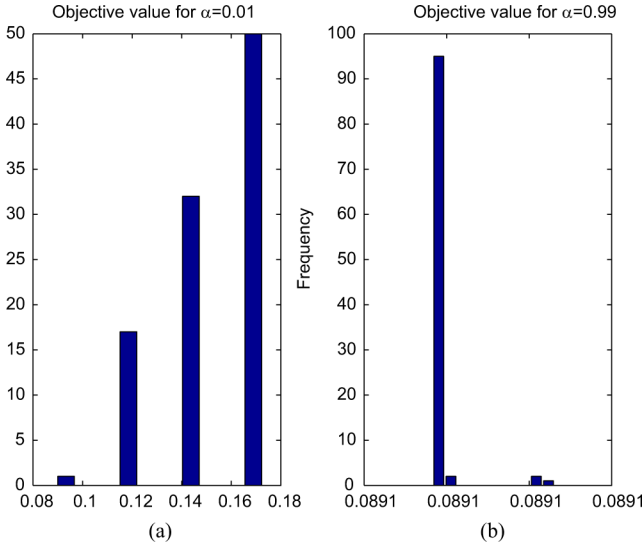


Fig. 3. Histograms of the objective values obtained when solving (13) 100 times with  $\alpha = 0.01$  (a) and  $\alpha = 0.99$  (b), for a given randomly generated square dictionary composed of 6 blocks of size 3. The sensing matrices of size  $12 \times 18$  are initialized as matrices with random entries. Note that the distribution is insignificant in (b), indicating that all the local minimum that our algorithm detected had the same objective value.

average recovery, all pairs of blocks in  $E$  should be as orthogonal as possible and also all pairs of atoms within each block should be as orthogonal as possible. Inspired by [8], rather than minimizing the interblock coherence  $\mu_B$  and the subblock coherence  $\nu$ , we aim at minimizing the *total interblock coherence*  $\mu_B^t$  and the *total subblock coherence*  $\nu^t$  of the equivalent dictionary  $E$ . We define the total interblock coherence as

$$\mu_B^t = \sum_{j=1}^B \sum_{i \neq j} \|G[i, j]\|_F^2 \quad (9)$$

and the total subblock coherence by

$$\nu^t = \sum_{j=1}^B \|G[j, j]\|_F^2 - \sum_{m=1}^K (G_m^m)^2 \quad (10)$$

where  $G_m^m$  are the diagonal entries of  $G$ . The total interblock coherence  $\mu_B^t$  equals the sum of the squared entries in  $G$  belonging to different blocks (the green entries in Fig. 1). Since this is the sum of Frobenius norms,  $\mu_B^t$  also equals the sum of the squared singular values of the cross-correlation blocks in  $G$ . When  $E$  is normalized,  $\mu_B^t$  is equivalent to the sum of the squared cosines of all the principal angles between all pairs of different blocks. The total subblock coherence  $\nu^t$  measures the sum of the squared off-diagonal entries belonging to the same block (the red entries in Fig. 1). When  $E$  is normalized,  $\nu^t$  equals the sum of the squared cosines of all the angles between atoms within the same block. Note that when the size of the blocks equals one, we get  $\nu^t = 0$ .

Alternatively, one could define the total interblock coherence as the sum of the squared spectral norms (i.e., the largest singular values) of the cross-correlation blocks in  $G$ , and the total subblock coherence as the sum of the squared maximal off-diagonal entries of the autocorrelation blocks in  $G$ . These definitions are closer to the ones used in (8). The WCM algorithm

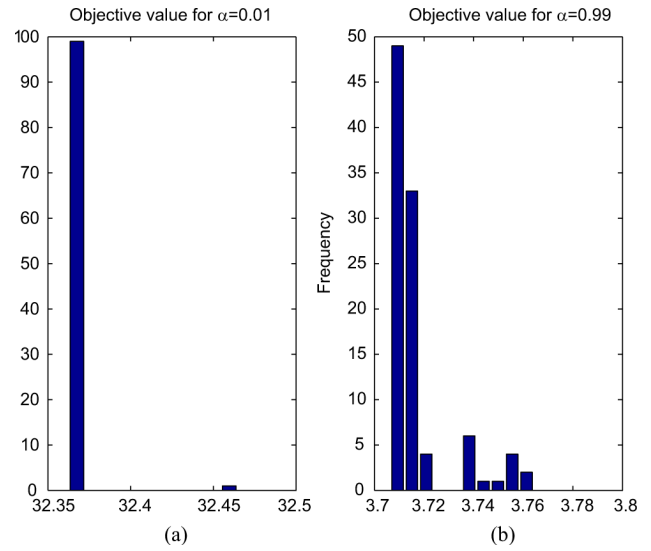


Fig. 4. Histograms of the objective values obtained when solving (13) 100 times with  $\alpha = 0.01$  (a) and  $\alpha = 0.99$  (b), for a given randomly generated overcomplete dictionary composed of 24 blocks of size 3. The sensing matrices of size  $12 \times 18$  are initialized as matrices with random entries.

presented in the next section can be slightly modified in order to minimize those measures as well. However, besides the increased complexity of the algorithm, the results appear to be inferior compared to minimizing the definitions (9) and (10) of  $\mu_B^t$  and  $\nu^t$ . This can be explained by the fact that maximizing only the smallest principal angle between pairs of different blocks in  $E$  and maximizing the smallest angle between atoms within the same block, creates a bulk of relatively high singular values and coherence values. While this may improve the worst-case bound in (8), it does not necessarily improve the average recovery ability of block-sparse approximation methods.

When minimizing the total interblock coherence and the total subblock coherence, we need to verify that the columns of  $E$  are normalized, to avoid the tendency of columns with small norm values to be underused. Rather than enforcing normalization strongly, we penalize for columns with norms that deviate from 1 by defining the *normalization penalty*  $\eta$

$$\eta = \sum_{m=1}^K (G_m^m - 1)^2. \quad (11)$$

This penalty  $\eta$  measures the sum of the squared distances between the diagonal entries in  $G$  (the yellow entries in Fig. 1) and 1.

While [8] did not deal with the block-sparse case, it is straightforward to see that solving (4) is equivalent to minimizing the sum of the normalization penalty, the total interblock coherence and the total subblock coherence

$$\begin{aligned} \|E'E - I\|_F^2 &= \sum_{j=1}^B \sum_{i \neq j} \|E[i]E[j]\|_F^2 + \sum_{j=1}^B \|E[j]E[j] - I\|_F^2 \\ &= \sum_{j=1}^B \sum_{i \neq j} \|G[i, j]\|_F^2 + \sum_{j=1}^B \|G[j, j] - I\|_F^2 \end{aligned}$$

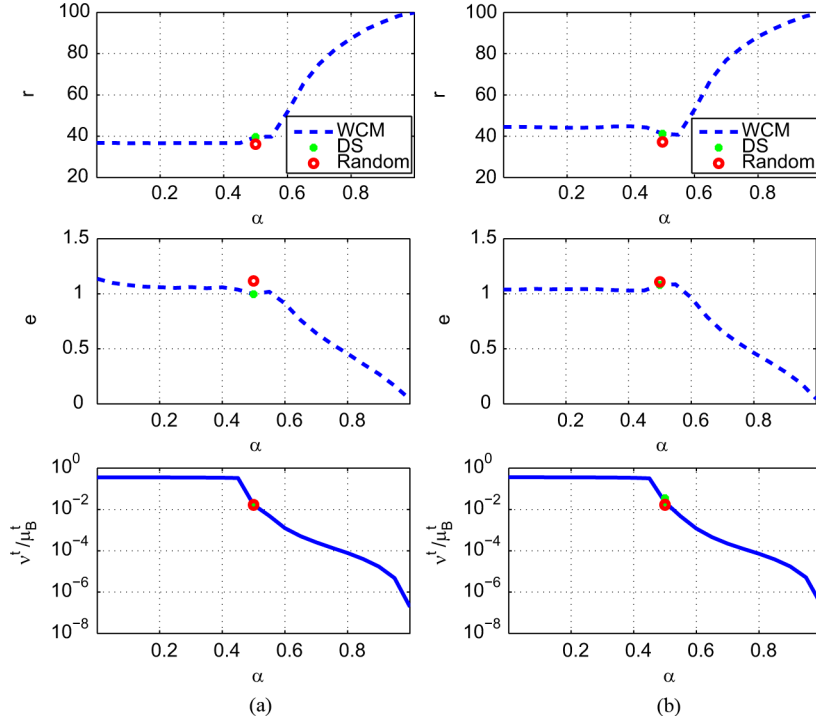


Fig. 5. Simulation results of sensing matrix design using the WCM algorithm with  $k = 1$  and  $M = 6$ . The graphs show the normalized representation error  $e$ , the classification success  $r$ , and the ratio between the total subblock coherence and the total interblock coherence  $\frac{\nu^t}{\mu_B^t}$  as a function of  $\alpha$ . In (a) the dictionary contains normally distributed entries, and in (b) randomly selected rows of the DCT matrix.

$$\begin{aligned}
 &= \sum_{j=1}^B \sum_{i \neq j} \|G[i, j]\|_F^2 + \sum_{j=1}^B \|G[j, j]\|_F^2 \\
 &\quad - \sum_{m=1}^K (G_m^m)^2 + \sum_{m=1}^K (G_m^m - 1)^2 \\
 &= \eta + \mu_B^t + \nu^t.
 \end{aligned}$$

We have shown in the previous section that the objective in (4) is bounded below by  $K - M$ . Therefore

$$\eta + \mu_B^t + \nu^t \geq K - M. \quad (12)$$

This bound implies a tradeoff, and as a consequence, one cannot minimize  $\eta$ ,  $\mu_B^t$ , and  $\nu^t$  freely. Instead, we propose designing a sensing matrix that minimizes the normalization penalty and a weighted sum of the total interblock coherence and the total subblock coherence

$$A = \arg \min_A \frac{1}{2} \eta + (1 - \alpha) \mu_B^t + \alpha \nu^t \quad (13)$$

where  $0 < \alpha < 1$  is a parameter controlling the weight given to the total interblock coherence and the total subblock coherence. Note that alternative objectives can be formulated. For example, one could add an additional weighting parameter to the normalization of the atoms in  $E$ , we prefer to deal with a single parameter only.

When  $\alpha < \frac{1}{2}$ , more weight is given to minimizing  $\mu_B^t$ , and therefore solving (13) leads to lower total interblock coherence,

which is made possible by aligning the atoms within each block [Fig. 2(a)]. On the other hand, choosing  $\alpha > \frac{1}{2}$  gives more weight to minimizing  $\nu^t$ . In this case, solving (13) leads to more orthonormal blocks in  $E$  at the expense of higher  $\mu_B^t$  [Fig. 2(c)]. Finally, setting  $\alpha = \frac{1}{2}$  in (13) gives equal weights to  $\mu_B^t$ ,  $\nu^t$ , and  $\eta$ , and reduces it to (4) [Fig. 2(b)]. Therefore, the objective becomes independent of the block structure, which makes  $\alpha = \frac{1}{2}$  the correct choice when the signals do not have an underlying block structure. Choosing to ignore the block structure leads to the same conclusion. When an underlying block structure exists, we need to select a value for  $\alpha$ . We do that via empirical evaluation in Section V.

In the next section we present an iterative algorithm that converges to a local solution of (13). Although we can only guarantee a local minimum, in our simulations we have noticed that independent executions of the algorithm tend to reach the same solution. Our empirical observations are demonstrated in the histograms in Fig. 3 (square dictionary) and Fig. 4 (a highly overcomplete dictionary), for both  $\alpha = 0.01$  and  $\alpha = 0.99$ .

#### IV. WCM—WEIGHTED COHERENCE MINIMIZATION

In this section, we present the WCM algorithm for minimizing (13), based on the bound-optimization method [26]. This algorithm substitutes the original objective with an easier to minimize surrogate objective that is updated in each optimization step. After defining a surrogate function and showing it can be minimized in closed form, we prove that its iterative minimization is guaranteed to converge to a local solution of the original problem.

### A. The WCM Algorithm

To obtain a surrogate function we rewrite the objective of (13), which we denote by  $f(G)$ , as a function of the Gram matrix of the equivalent dictionary  $G = D'A'AD$

$$\begin{aligned} f(G) &\equiv \frac{1}{2}\eta(G) + (1 - \alpha)\mu_B^t(G) + \alpha\nu^t(G) \\ &= \frac{1}{2}\|u_\eta(G)\|_F^2 + (1 - \alpha)\|u_\mu(G)\|_F^2 + \alpha\|u_\nu(G)\|_F^2 \end{aligned}$$

where the matrix operators  $u_\mu$ ,  $u_\nu$ , and  $u_\eta$  are defined as

$$\begin{aligned} u_\eta(G)[i, j]_n^m &= \begin{cases} G[i, j]_n^m - 1, & i = j, m = n; \\ 0, & \text{else,} \end{cases} \\ u_\mu(G)[i, j]_n^m &= \begin{cases} G[i, j]_n^m, & i \neq j; \\ 0, & \text{else,} \end{cases} \\ u_\nu(G)[i, j]_n^m &= \begin{cases} G[i, j]_n^m, & i = j, m \neq n; \\ 0, & \text{else} \end{cases} \end{aligned}$$

with  $G[i, j]_n^m$  denoting the  $(m, n)$ th entry of  $G[i, j]$ . This equation follows directly from the definitions of  $\eta$ ,  $\mu_B^t$ , and  $\nu^t$ . We can now write

$$f(G) = \frac{1}{2}\|G - h_\eta(G)\|_F^2 + (1 - \alpha)\|G - h_\mu(G)\|_F^2 + \alpha\|G - h_\nu(G)\|_F^2 \quad (14)$$

where the matrix operators  $h_\mu$ ,  $h_\nu$ , and  $h_\eta$  are defined as

$$\begin{aligned} h_\eta(G)[i, j]_n^m &= \begin{cases} 1, & i = j, m = n; \\ G[i, j]_n^m, & \text{else,} \end{cases} \\ h_\mu(G)[i, j]_n^m &= \begin{cases} 0, & i \neq j; \\ G[i, j]_n^m, & \text{else,} \end{cases} \\ h_\nu(G)[i, j]_n^m &= \begin{cases} 0, & i = j, m \neq n; \\ G[i, j]_n^m, & \text{else.} \end{cases} \end{aligned}$$

Based on (14), we define a surrogate objective  $g(G, G^{(n)})$  at the  $n$ th iteration as

$$\begin{aligned} g(G, G^{(n)}) &\equiv \frac{1}{2}\|G - h_\eta(G^{(n)})\|_F^2 \\ &+ (1 - \alpha)\|G - h_\mu(G^{(n)})\|_F^2 + \alpha\|G - h_\nu(G^{(n)})\|_F^2 \quad (15) \end{aligned}$$

where  $G^{(n)} = D'A^{(n)'}A^{(n)}D$  is the Gram matrix of the equivalent dictionary from the previous iteration. In Appendix B, we prove that  $g(G, G^{(n)})$  satisfies the conditions of a surrogate objective for the bound-optimization method. Therefore, iteratively minimizing  $g(G, G^{(n)})$  is guaranteed to converge to a local minimum of the original objective  $f(G)$ , i.e., solve (13).

The following proposition describes the closed form solution to minimizing  $g(G, G^{(n)})$  at each iteration.

*Proposition 1:* The function  $g(G, G^{(n)})$  is minimized by choosing

$$A^{(n+1)} = \Delta_M^{-\frac{1}{2}} V_M' \Lambda^{-\frac{1}{2}} U'$$

where  $U\Lambda U'$  is the eigenvalue decomposition of  $DD'$ ,  $\Delta_M$ , and  $V_M$  are the top  $M$  eigenvalues and the corresponding  $M$  eigenvectors of  $\Lambda^{-\frac{1}{2}} U' D h_t(G^{(n)}) D' U \Lambda^{-\frac{1}{2}}$ , and

$$h_t(\cdot) \equiv \frac{2}{3} \left( \frac{1}{2} h_\eta(\cdot) + (1 - \alpha) h_\mu(\cdot) + \alpha h_\nu(\cdot) \right). \quad (16)$$

*Proof:* See Appendix B ■

A summary of the proposed WCM algorithm is given below. The computation complexity of this algorithm is  $O(N^3)$ . This is since every iteration includes finding the  $M$  principal components of an  $N \times N$  matrix (the sensing matrix  $A$  is in  $M \times N$ ), i.e., SVD of complexity  $N^3$ .

---

### Algorithm 1: Weighted Coherence Minimization

---

*Task:* Solve for a given block-sparsifying dictionary  $D_{N \times K}$

$$A = \arg \min_A \frac{1}{2}\eta + (1 - \alpha)\mu_B^t + \alpha\nu^t$$

where  $A \in R^{M \times N}$ .

*Initialization:* Calculate the eigenvalue decomposition of  $DD' = U\Lambda U'$ . Set  $A^{(0)}$  as the outcome of (4), i.e.,  $A^{(0)} = [I_M \ 0]\Lambda^{-\frac{1}{2}}U'$ , and  $n = 0$ .

*Repeat until convergence:*

- 1) Set  $G^{(n)} = D'A^{(n)'}A^{(n)}D$ .
  - 2) Calculate  $h_t(G^{(n)})$  as in (16).
  - 3) Find the top  $M$  eigenvalues  $\Delta_M$  and the corresponding  $M$  eigenvectors  $V_M$  of  $\Lambda^{-\frac{1}{2}}U'Dh_t(G^{(n)})D'U\Lambda^{-\frac{1}{2}}$ .
  - 4) Set  $A^{(n+1)} = \Delta_M^{-\frac{1}{2}}V_M'\Lambda^{-\frac{1}{2}}U'$ .
  - 5)  $n = n + 1$
- 

## V. EXPERIMENTS

In this section, we evaluate the contribution of the proposed sensing matrix design framework empirically. We compare the recovery and classification abilities of BOMP [24], [25] when using sensing matrices designed by the proposed WCM to the outcome of (4), which will be referred to as ‘‘Duarte-Sapiro’’ (DS) [8].

### A. Experiments on Synthetic Data

For each simulation, we repeat the following procedure 100 times. We randomly generate a dictionary  $D_{N \times K}$  with normally distributed entries and normalize its columns. In order to evaluate WCM on structured dictionaries as well, we repeat the simulations using a dictionary containing  $N$  randomly selected rows of the  $K \times K$  Discrete Cosine Transform (DCT) matrix. The dictionary is divided into  $\frac{K}{s}$  blocks of size  $s$ . We then generate  $L = 1000$  test signals  $X$  of dimension  $K$  that have  $k$  block-sparse representations  $\Theta$  with respect to  $D$ . The generating blocks are chosen randomly and independently and the coefficients are i.i.d. uniformly distributed. We compare three options for designing  $A_{M \times N}$ : (i) random; (ii) the outcome of DS; and (iii) the proposed WCM which is initialized as the outcome of DS. Having found  $A$  we calculate the equivalent dictionary  $E = AD$  and the measurements  $Y = AX$ . Next, we obtain the block-sparsest representations of the measurements,  $\hat{\Theta}$ , by applying BOMP with a fixed number of  $k$  nonzero blocks.

We use two measures to evaluate the success of the simulations based on their outputs  $A$  and  $\hat{\Theta}$ .

- The percentage of recognized generating subspaces of  $X$  (i.e., successful classification):  $r = \frac{\|\hat{\Theta} \odot \Theta\|_0}{Lks}$  where  $\odot$  denotes element-wise multiplication.

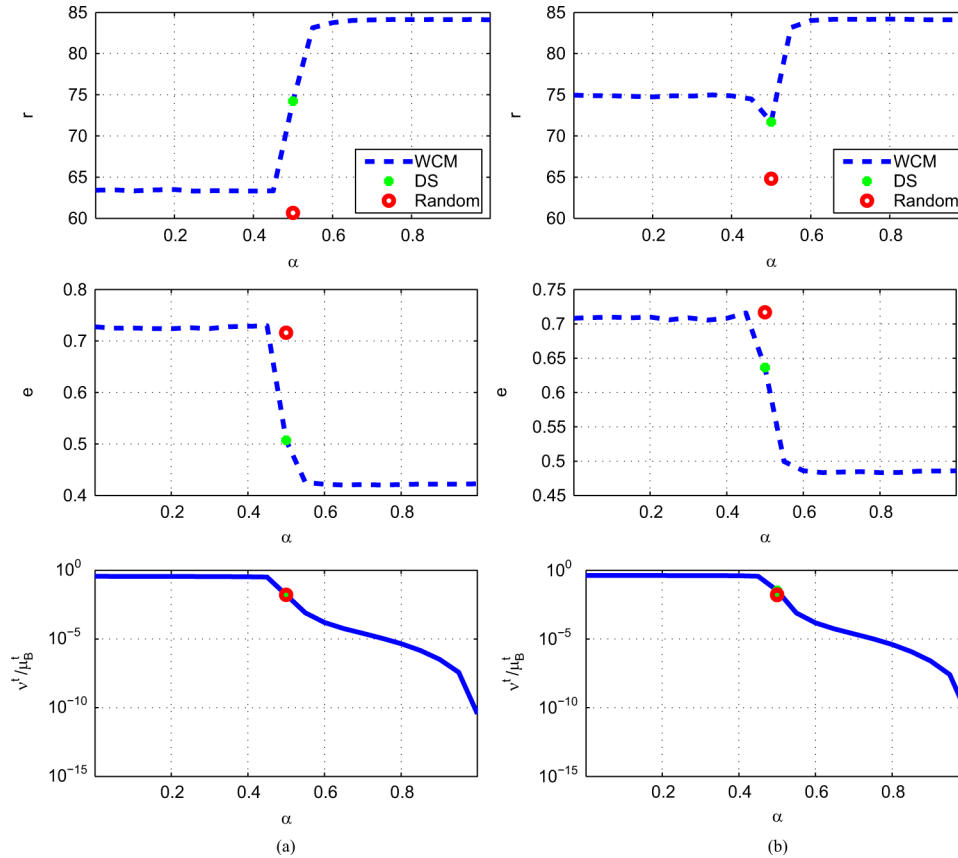


Fig. 6. Simulation results of sensing matrix design using the WCM algorithm with  $k = 2$  and  $M = 14$ . The graphs show the normalized representation error  $e$ , the classification success  $r$ , and the ratio between the total subblock coherence and the total interblock coherence  $\frac{\nu^t}{\mu_B^t}$  as a function of  $\alpha$ . In (a) the dictionary contains normally distributed entries, and in (b) randomly selected rows of the DCT matrix.

- The normalized representation error  $e = \frac{\|X - D\hat{\Theta}\|_F}{\|X\|_F}$ .

**Tuning  $\alpha$ :** To evaluate the performance of the WCM algorithm as a function of  $\alpha$ , we choose  $s = 3$ ,  $N = 60$  and  $K = 2N = 120$ . We repeat the experiment for both types of dictionaries, and for  $k = 1$  [Fig. 5(a) and (b)],  $k = 2$  [Fig. 6(a) and (b)] and  $k = 3$  [Fig. 7(a) and (b)] nonzero blocks, with, respectively,  $M = 6$ ,  $M = 14$ , and  $M = 20$  measurements. To show that the results remain consistent for higher values of  $k$ , we add an experiment with  $k = 6$ ,  $M = 35$ ,  $N = 180$ , and  $K = 2N = 360$  [Fig. 8(a) and (b)]. We compare the obtained results to randomly set sensing matrices and to the outputs of DS [8], based on the normalized representation error  $e$ , the classification success  $r$ , and the ratio between the total subblock coherence and the total interblock coherence  $\frac{\nu^t}{\mu_B^t}$ .

The results indicate that WCM and DS coincide at  $\alpha = 0.5$  for all the three measures, as expected. Note that for  $\alpha < 0.5$  we get that  $\frac{\nu^t}{\mu_B^t}$  is high,  $e$  is high, and  $r$  is low. On the other hand, when  $\alpha > 0.5$ , i.e., when giving more weight to  $\nu^t$  and less to  $\mu_B^t$ , the signal reconstruction as well as the signal classification are improved compared to DS. This is in line with our earlier observation based on the bound in (8) that the ratio  $\frac{\nu^t}{\mu_B^t}$  should be small. Indeed our experiments show that when  $\alpha > 0.5$  we get that  $\frac{\nu^t}{\mu_B^t}$  is low. The simulation results show a dramatic change in performance around the value  $\alpha = 0.5$ . This is since at  $\alpha = 0.5$  the importance of  $\nu^t$  becomes higher than that of  $\mu_B^t$ , which changes the behavior of the algorithm.

While the improvement for  $k = 1$  is more significant, it is maintained for higher values of  $k$  as well. Remarkably, for structured dictionaries and for higher values of  $k$ , we see that  $\alpha < 0.5$  leads to an improvement of  $r$ . However,  $e$  is compromised in this case. We can conclude that when designing sensing matrices for block sparse decoding, the best results are obtained by choosing  $\alpha$  close enough to 1. In other words, the best recovery results are obtained when the equivalent dictionary has nearly orthonormal blocks. This holds for dictionaries containing normally distributed entries as well as for dictionaries containing randomly selected rows of the DCT matrix. When the dictionary is overcomplete the blocks cannot be truly orthonormal. Based on these observations we conclude that  $\alpha \approx 1$  is the best value. In our experiments on real data (next section) setting  $\alpha = 1$  led to the same results as values close to 1. However, we did not want to completely ignore the interblock coherence thus we typically set  $\alpha = 0.99$ .

As mentioned before, WCM converges but could get trapped in local minima. As was shown in Fig. 3(b), we observed empirically that for  $\alpha > 0.5$ , every local minimum reached had the same objective value. We observed this empirical behavior also in the exhaustive experiments presented in this section. This means that the WCM algorithm converges consistently to the same solution of (13) when  $\alpha > 0.5$ , for all the experiments presented in this section. We emphasize however, that this may not be the case for other sets of parameters.

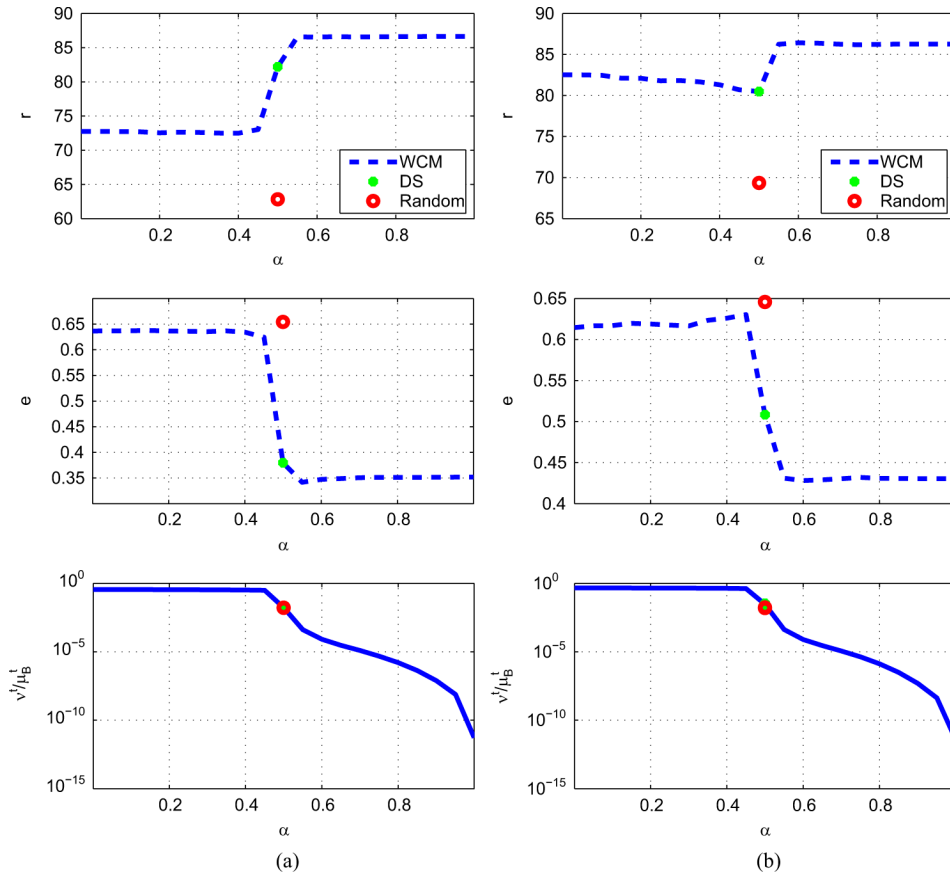


Fig. 7. Simulation results of sensing matrix design using the WCM algorithm with  $k = 3$  and  $M = 20$ . The graphs show the normalized representation error  $e$ , the classification success  $r$ , and the ratio between the total subblock coherence and the total interblock coherence  $\frac{\mu_B^t}{\mu_B^k}$  as a function of  $\alpha$ . In (a) the dictionary contains normally distributed entries, and in (b) randomly selected rows of the DCT matrix.

**Dictionary dimension:** Fig. 9(a) and (b) shows that when using WCM with  $\alpha = 0.99$  on dictionaries with normally distributed entries and on structured dictionaries, the improvement in signal recovery is maintained for a wide range of  $K$ , starting from square dictionaries, i.e.,  $K = N$ , to highly overcomplete dictionaries. For this experiment, we chose  $s = 3$ ,  $N = 60$ ,  $k = 2$  and  $M = 14$ . We note that for both types of dictionaries, the improvement of WCM over DS increases as the dictionary becomes more over-complete.

**Varying block sizes:** Finally, we show that WCM improves the results of block-sparse decoding for dictionaries with blocks of varying sizes as well. The generated dictionaries contain 15 blocks of size 4 and 20 blocks of size 3, with  $N = 60$  and  $K = 2N = 120$ . In this example, we set  $k = 2$  and  $M = 14$ . The results are shown as a function of  $\alpha$  in Fig. 10(a) for dictionaries with normally distributed entries and in Fig. 10(b) for structured dictionaries.

### B. Experiments on Real Image Data

To evaluate the applicability of the proposed approach in practical scenarios we further perform experiments on real image data. Similar to [8] we experimented with compression of image patches. We begin by hand-crafting a block-sparse dictionary  $D$ . We select  $B = 50$  random locations in a given training image [Fig. 11(a)] and extract around each location 9 overlapping patches of size  $7 \times 7$ , which are reshaped into 49

dimensional column vectors. We then fit a linear subspace of dimension  $s = 6$  to each group of overlapping patches. The computed 50 subspaces are used to construct our dictionary  $D$  (i.e.,  $K = 300$ ).

We then take 500 different testing images [see an example in Fig. 11(b)] and extract from each image all the nonoverlapping patches of size  $7 \times 7$ , which are reshaped into 49 dimensional column vectors. They are compressed into  $M = 15$  dimensions using a sensing matrix  $A_{M \times N}$ . Three sensing matrices are tested: (i) random; (ii) designed according to DS [8]; and (iii) designed according to our WCM algorithm with  $\alpha = 0.99$ . Next, we obtain the block-sparse representations  $\Theta$  of the signals by applying BOMP with a fixed number of  $k = 2$  nonzero blocks. The sparse representations  $\Theta$  are used to recover the original signals of size 49. We then compute the mean representation over all image patches. For presentation purposes, we further reshape the estimated signals into  $7 \times 7$  patches and reconstruct the image.

The above procedure was repeated 10 times, for 10 different dictionaries (each obtained using a different random selection of the training subspaces). Fig. 11(c) presents the mean representation error over the 10 trials for each of the 500 testing images. WCM consistently leads to smaller errors.

Next, we repeat the same experiment but replacing the hand-crafted dictionary with one trained using the approach proposed in [27]. To train the dictionary we extract all  $7 \times 7$  patches from



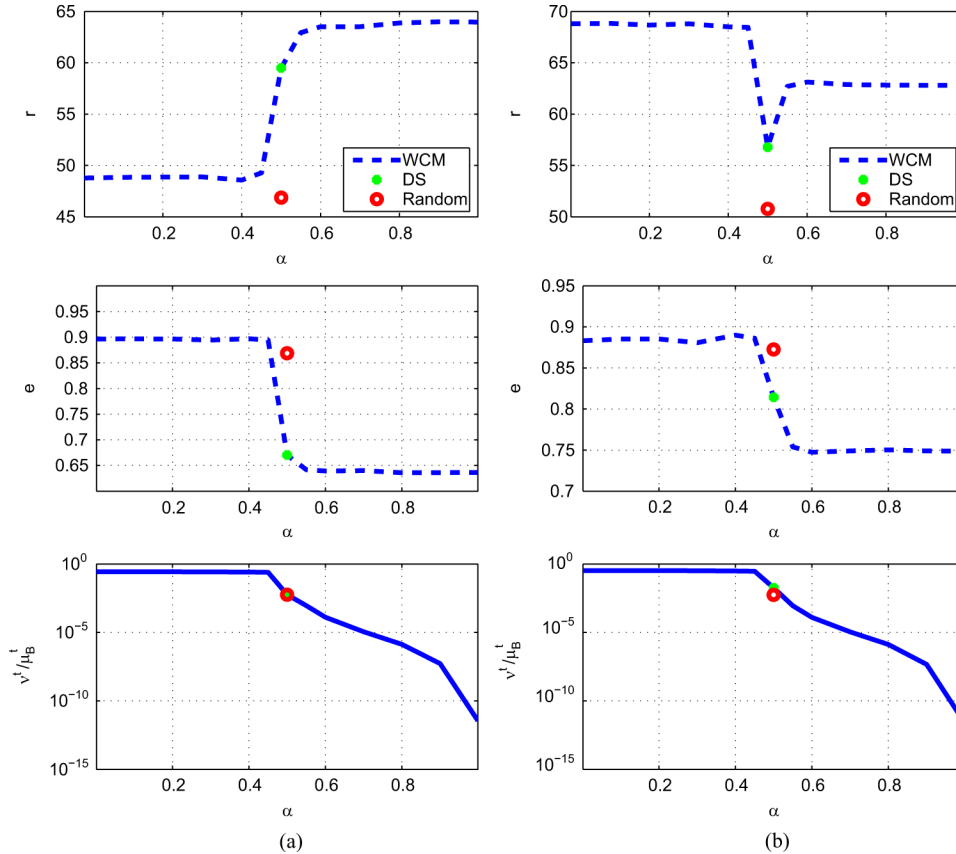


Fig. 8. Simulation results of sensing matrix design using the WCM algorithm with  $k = 6$  and  $M = 35$ . The graphs show the normalized representation error  $e$ , the classification success  $r$ , and the ratio between the total subblock coherence and the total interblock coherence  $\frac{v^t}{\mu_B^t}$  as a function of  $\alpha$ . In (a) the dictionary contains normally distributed entries, and in (b) randomly selected rows of the DCT matrix.

the training image (total of 294). We then use SAC+BKSVD (see [27]) to train the dictionary  $D$  and recover the block structure. The rest of the experiment remains the same. As shown in Fig. 11(g)–(i), using the trained dictionary instead of the designed one has little effect on the results.

Finally, we further evaluate the results as a function of  $\alpha$ . Fig. 12 demonstrates that the results on image compression. When  $\alpha > 0.5$  the reconstruction error is smaller for WCM than for DS or for a random  $A$ . Note, that this is true for both  $k = 1$  and  $k = 2$ , however, the improvement for  $k = 2$  is more significant.

## VI. CONCLUSION

In this paper, we proposed a framework for the design of a sensing matrix, assuming that a block-sparsifying dictionary is provided. We minimize a weighted sum of the total interblock coherence and the total subblock coherence, while attempting to keep the atoms in the equivalent dictionary as normalized as possible [see (13)]. This objective can be seen as an intuitive extension of (4) to the case of blocks.

While it might be possible to derive a closed form solution to (13), we have presented the Weighted Coherence Minimization algorithm, an elegant iterative solution which is based on the bound-optimization method. In this method, the original objective is replaced with an easier to solve surrogate objective in

each step. This algorithm eventually converges to a local solution of (13).

Simulations have shown that the best results are obtained when minimizing mostly the total subblock coherence. This leads to equivalent dictionaries with nearly orthonormal blocks, at the price of a slightly increased total interblock coherence. The obtained sensing matrix outperforms the one obtained when using the DS algorithm [8] to solve (4). This improvement manifests itself in lower signal reconstruction errors and higher rates of successful signal classification. When giving equal weight to the total interblock coherence and to the total subblock coherence, the results are identical to solving (4). Moreover, both objectives coincide for this specific choice of  $\alpha$ , which ignores the existence of a block structure in the sparse representations of the signal data.

## APPENDIX A PROOF OF CONVERGENCE

The surrogate function  $g(G, G^{(n)})$  has been chosen in such a way as to bound the original objective  $f(G)$  from above for every  $G$ , and to coincide at  $G = G^{(n)}$ . Minimizing  $g(G, G^{(n)})$  will then necessarily decrease the value of  $f(G)$

$$\begin{aligned} \min_G g(G, G^{(n)}) &\leq g(G^{(n)}, G^{(n)}) = f(G^{(n)}), \\ f(G^{(n+1)}) &\leq g(G^{(n+1)}, G^{(n)}) = \min_G g(G, G^{(n)}). \end{aligned}$$

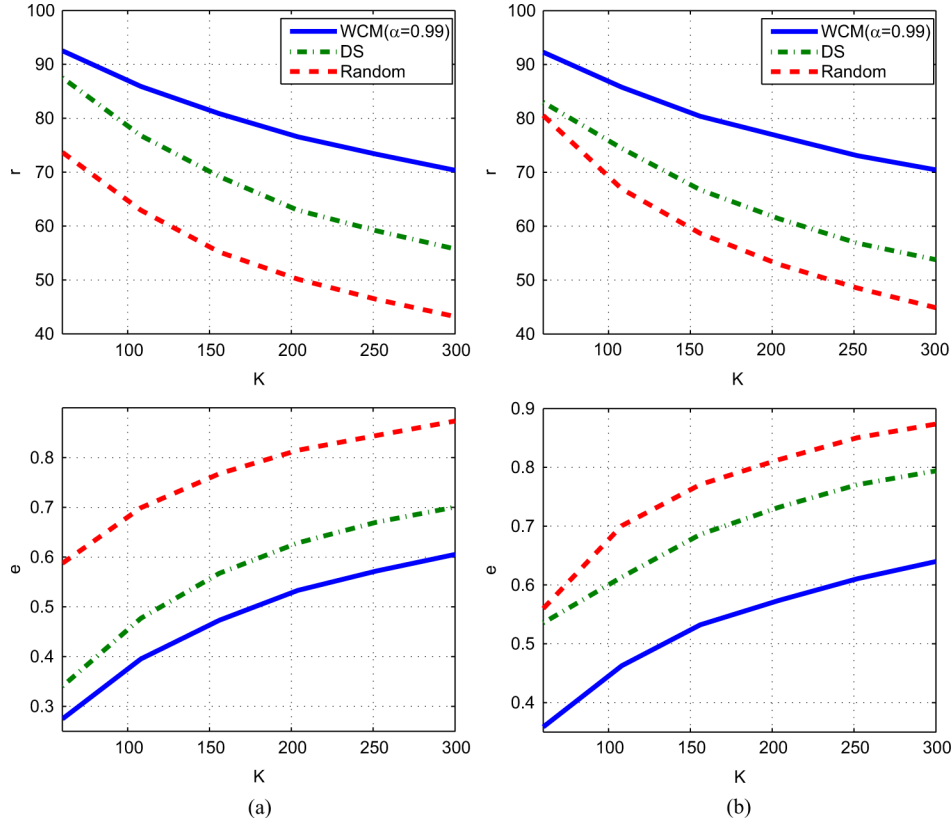


Fig. 9. Simulation results of sensing matrix design using the WCM algorithm with  $k = 2$  and  $M = 14$ . The graphs show the normalized representation error  $\epsilon$  and the classification success  $r$  as a function of  $K$ . In (a) the dictionary contains normally distributed entries, and in (b) randomly selected rows of the DCT matrix.

Formally, according to [26], the sequence of solutions generated and by iteratively solving

$$G^{(n+1)} = \arg \min_G g(G, G^{(n)}) \quad (17)$$

is guaranteed to converge to a local minimum of the original objective  $f(G)$  when the surrogate objective  $g(G, G^{(n)})$  satisfies the following three constraints:

1) **Equality at  $G = G^{(n)}$ :**

$$g(G^{(n)}, G^{(n)}) = f(G^{(n)}).$$

2) **Upper-bounding the original function:**

$$g(G, G^{(n)}) \geq f(G), \forall G.$$

3) **Equal gradient at  $G = G^{(n)}$ :**

$$\nabla g(G, G^{(n)})|_{G=G^{(n)}} = \nabla f(G)|_{G=G^{(n)}}.$$

We next prove that the three conditions hold.

*Proof: Equality at  $G = G^{(n)}$ :* This follows from the definition of  $g(G, G^{(n)})$ .

**Upper-bounding the original function:** Let us rewrite both functions  $g(G, G^{(n)})$  and  $f(G)$  using the definition of the Frobenius norm

$$\begin{aligned} g(G, G^{(n)}) &= \sum_{i,j} \sum_{m,n} \left[ \frac{1}{2} ((G - h_\eta(G^{(n)}))[i, j]_n^m)^2 \right. \\ &\quad + (1 - \alpha) ((G - h_\mu(G^{(n)}))[i, j]_n^m)^2 \\ &\quad \left. + \alpha ((G - h_\nu(G^{(n)}))[i, j]_n^m)^2 \right], \end{aligned}$$

$$\begin{aligned} f(G) &= \sum_{i,j} \sum_{m,n} \left[ \frac{1}{2} (u_\eta(G)[i, j]_n^m)^2 \right. \\ &\quad + (1 - \alpha) (u_\mu(G)[i, j]_n^m)^2 \\ &\quad \left. + \alpha (u_\nu(G)[i, j]_n^m)^2 \right]. \end{aligned}$$

The following observations prove that each of the terms in  $g(G, G^{(n)})$  is larger than or equal to its counterpart in  $f(G)$ , and therefore  $g(G, G^{(n)}) \geq f(G)$ :

$$\begin{aligned} u_\eta(G)[i, j]_n^m &= \begin{cases} G[i, j]_n^m - 1, & i = j, m = n; \\ 0, & \text{else.} \end{cases} \\ (G - h_\eta(G^{(n)}))[i, j]_n^m &= \begin{cases} G[i, j]_n^m - 1, & i = j, \\ & m = n; \\ (G - G^{(n)})[i, j]_n^m, & \text{else.} \end{cases} \\ u_\mu(G)[i, j]_n^m &= \begin{cases} G[i, j]_n^m, & i \neq j; \\ 0, & \text{else.} \end{cases} \\ (G - h_\mu(G^{(n)}))[i, j]_n^m &= \begin{cases} G[i, j]_n^m, & i \neq j; \\ (G - G^{(n)})[i, j]_n^m, & \text{else.} \end{cases} \\ u_\nu(G)[i, j]_n^m &= \begin{cases} G[i, j]_n^m, & i = j, m \neq n; \\ 0, & \text{else.} \end{cases} \\ (G - h_\nu(G^{(n)}))[i, j]_n^m &= \begin{cases} G[i, j]_n^m, & i = j, \\ & m \neq n; \\ (G - G^{(n)})[i, j]_n^m, & \text{else.} \end{cases} \end{aligned}$$

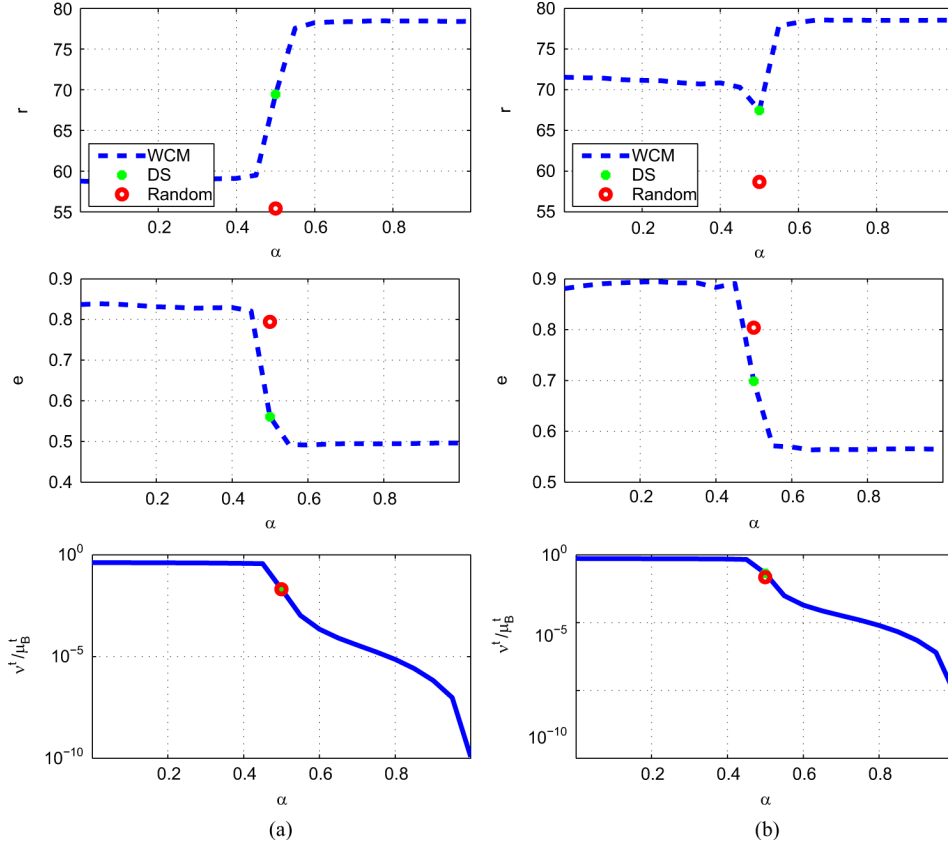


Fig. 10. Simulation results of sensing matrix design using the WCM algorithm on a dictionary containing 15 blocks of size 4 and 20 blocks of size 3, with  $k = 2$  and  $M = 14$ . The graphs show the normalized representation error  $e$ , the classification success  $r$ , and the ratio between the total subblock coherence and the total interblock coherence  $\frac{v^t}{\mu_B^t}$  as a function of  $\alpha$ . In (a) the dictionary contains normally distributed entries, and in (b) randomly selected rows of the DCT matrix.

**Equal gradient at  $G = G^{(n)}$ :** We calculate the gradient of  $g(G, G^{(n)})$  and  $f(G)$

$$\begin{aligned} \nabla g(G, G^{(n)}) &= 2 \left[ \frac{1}{2}(G - h_\eta(G^{(n)})) \right. \\ &\quad + (1 - \alpha)(G - h_\mu(G^{(n)})) \\ &\quad \left. + \alpha(G - h_\nu(G^{(n)})) \right] \\ \nabla f(G) &= 2 \left[ \frac{1}{2}u_\eta(G) + (1 - \alpha)u_\mu(G) + \alpha u_\nu(G) \right]. \end{aligned}$$

When substituting  $G = G^{(n)}$  we obtain

$$\begin{aligned} \nabla g(G, G^{(n)})|_{G=G^{(n)}} &= \nabla f(G)|_{G=G^{(n)}} \\ &= 2 \left( \frac{1}{2}u_\eta(G^{(n)}) + (1 - \alpha)u_\mu(G^{(n)}) + \alpha u_\nu(G^{(n)}) \right). \end{aligned}$$

Therefore, the gradients of both objectives coincide at  $G = G^{(n)}$ . This completes the convergence proof.

## APPENDIX B PROOF OF PROPOSITION 1

*Proof:* In order to minimize  $g(G, G^{(n)})$ , we rewrite the problem in an alternative form

$$\begin{aligned} &\min_A g(G, \cdot) \\ &= \min_A \text{tr} \left( \frac{3}{2}G'G - 2G' \left[ \frac{1}{2}h_\eta(\cdot) + (1 - \alpha)h_\mu(\cdot) + \alpha h_\nu(\cdot) \right] \right) \\ &= \min_A \text{tr}(E'EE'E - 2E'Eh_t(\cdot)) \\ &= \min_A \text{tr}(EE'EE' - 2Eh_t(\cdot)E') \\ &= \min_A \text{tr}(ADD'A'ADD'A' - 2ADh_t(\cdot)D'A') \quad (18) \end{aligned}$$

where  $h_t(\cdot)$  is defined in (16). Let  $UAU'$  be the eigenvalue decomposition of  $DD'$  and define  $\Gamma_{M \times N} = AU\Lambda^{\frac{1}{2}}$ . Substituting into (18) yields

$$\begin{aligned} &\min_A g(G, \cdot) \\ &= \min_A \text{tr}(\Gamma\Gamma'\Gamma\Gamma' - 2\Gamma\Lambda^{-\frac{1}{2}}U'Dh_t(\cdot)D'U\Lambda^{-\frac{1}{2}}\Gamma') \\ &= \min_A \|\Gamma\Gamma' - \tilde{h}_t(\cdot)\|_F^2 \quad (19) \end{aligned}$$

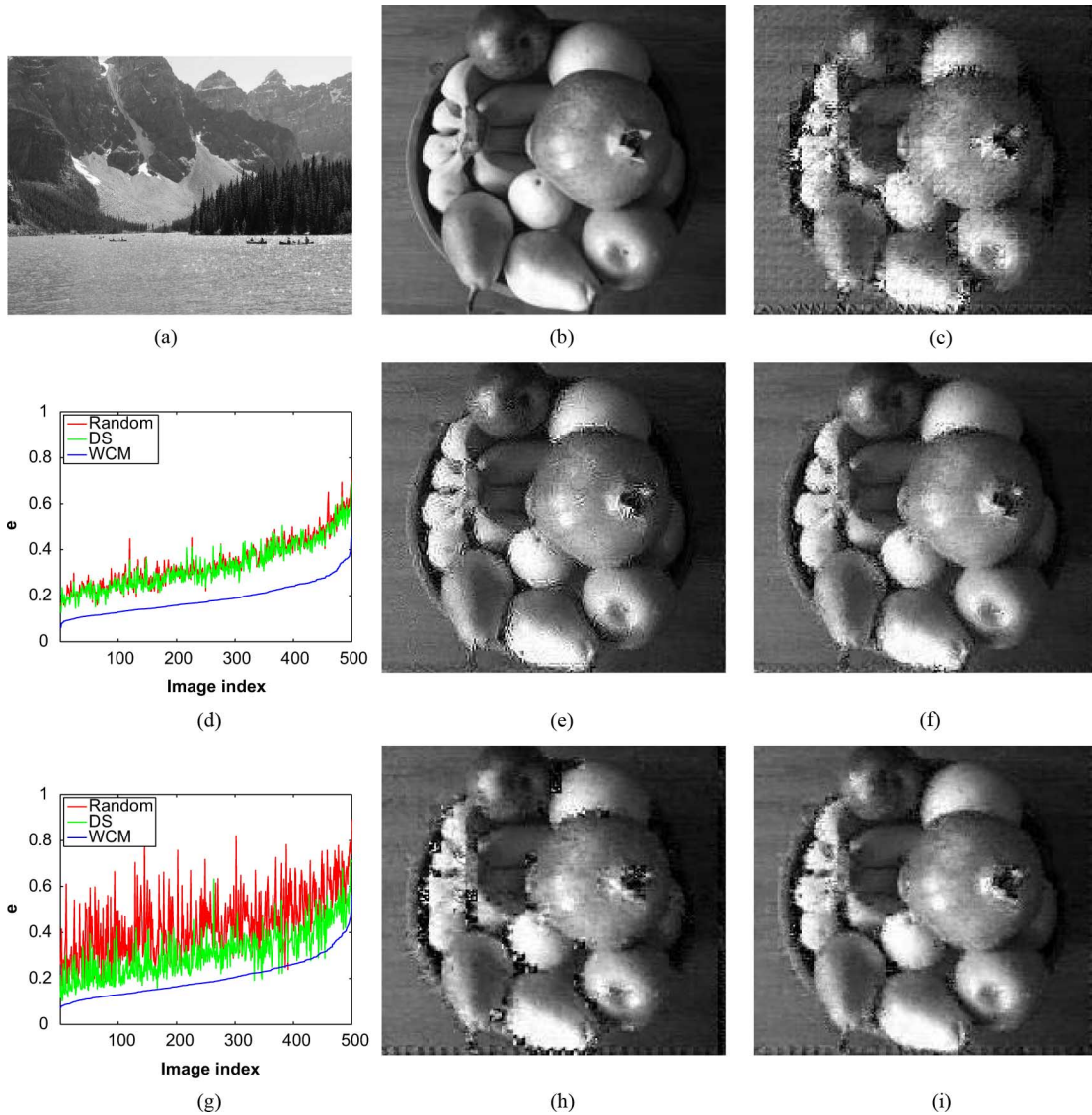


Fig. 11. Image compression experiment (a) An image used to train sensing matrices using DS and WCM (b) An example of a query image (500 total) that was decomposed into  $7 \times 7$  nonoverlapping patches which were compressed into 15 dimensions using each of the sensing matrices. We then use BOMP to recover the sparse representation of the original patches and reconstruct them. (d,g) Representation errors for each of the 500 different query images. WCM leads to smallest errors on almost all the images. (c,e,f,h,i) The obtained reconstructions (a) Training image. (b) An example query image. (c) Random  $A$ . (d) Representation error  $D$  designed. (e)  $A$  trained by DS  $D$  designed. (f)  $A$  trained by WCM  $D$  designed. (g) Representation error,  $D$  trained by [27]. (h)  $A$  trained by DS  $D$  trained by [27]. (i)  $A$  trained by WCM  $D$  trained by [27].

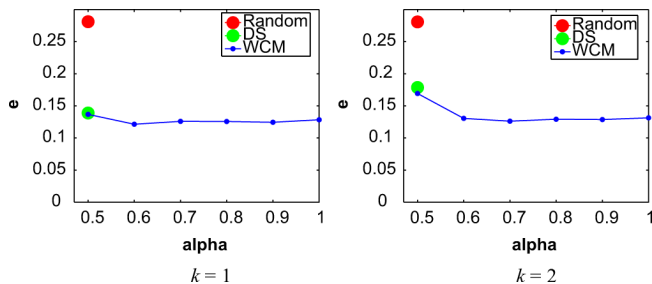


Fig. 12. Repeating the experiment of Fig. 11 for varying values of  $\alpha$ . When  $\alpha > 0.5$  WCM results in lower errors compared to DS and random  $A$ .

where  $\tilde{h}_t(\cdot) \equiv \Lambda^{-\frac{1}{2}} U' D h_t(\cdot) D' U \Lambda^{-\frac{1}{2}}$ . According to (19), the surrogate objective  $g(G, G^{(n)})$  can be minimized in closed form by finding the top  $M$  components of  $\tilde{h}_t(G^{(n)})$ . Let  $\Delta_M$  be the

top  $M$  eigenvalues of  $\tilde{h}_t(G^{(n)})$  and  $V_M$  the corresponding  $M$  eigenvectors. Then, (19) is solved by setting  $\Gamma = \Delta_M^{\frac{1}{2}} V_M'$ . Note that this solution is not unique, since  $\Gamma$  can be multiplied on the left by any unitary matrix. This, however, does not affect the WCM algorithm since we only care about updating the Gram matrix  $G^{(n+1)}$ , which is not influenced by the multiplication of  $A^{(n+1)}$  on the left by a unitary matrix. Finally, the optimal sensing matrix is given by  $A^{(n+1)} = \Gamma \Lambda^{-\frac{1}{2}} U' = \Delta_M^{\frac{1}{2}} V_M' \Lambda^{-\frac{1}{2}} U'$ .

## REFERENCES

- [1] E. Candes, J. Romberg, and T. Tao, "Robust uncertainty principles: Exact signal reconstruction from highly incomplete frequency information," *IEEE Trans. Inf. Theory*, vol. 52, pp. 489–509, Feb. 2006.
- [2] D. Donoho, "Compressed sensing," *IEEE Trans. Inf. Theory*, vol. 52, no. 4, pp. 1289–1306, Apr. 2006.

- [3] S. S. Chen, D. L. Donoho, and M. A. Saunders, "Atomic decomposition by basis pursuit," *SIAM J. Sci. Comput.*, vol. 20, no. 1, pp. 33–61, 1999.
- [4] J. Tropp, "Greed is good: Algorithmic results for sparse approximation," *IEEE Trans. Inf. Theory*, vol. 50, no. 10, pp. 2231–2242, Oct. 2004.
- [5] S. G. Mallat and Z. Zhang, "Matching pursuits and time-frequency dictionaries," *IEEE Trans. Signal Process.*, vol. 41, no. 12, pp. 3397–3415, Dec. 1993.
- [6] Y. Weiss, H. S. Chang, and W. T. Freeman, "Learning compressed sensing," in *Proc. Allerton Conf.*, Sep. 2007.
- [7] M. Elad, "Optimized projections for compressed sensing," *IEEE Trans. Signal Process.*, vol. 55, no. 12, pp. 5695–5702, Dec. 2007.
- [8] J. M. Duarte-Carvajalino and G. Sapiro, "Learning to sense sparse signals: Simultaneous sensing matrix and sparsifying dictionary optimization," *IMA Preprint Ser.*, no. 2211, May 2008.
- [9] Y. M. Lu and M. N. Do, "A theory for sampling signals from a union of subspaces," *IEEE Trans. Signal Process.*, vol. 56, no. 6, pp. 2334–2345, Jun. 2008.
- [10] K. Gedalyahu and Y. C. Eldar, "Time delay estimation from low rate samples: A union of subspaces approach," *IEEE Trans. Signal Process.*, vol. 58, no. 6, pp. 3017–3031, Jun. 2010.
- [11] Y. C. Eldar and M. Mishali, "Robust recovery of signals from a structured union of subspaces," *IEEE Trans. Inf. Theory*, vol. 55, no. 11, pp. 5302–5316, Nov. 2009.
- [12] R. Basri and D. Jacobs, "Lambertian reflectances and linear subspaces," *IEEE Trans. Pattern Anal. Machine Intell.*, vol. 25, no. 2, pp. 383–390, Feb. 2003.
- [13] A. Y. Yang, J. Wright, Y. Ma, and S. Sastry, "Feature Selection in Face Recognition: A Sparse Representation Perspective," Univ. of California Berkeley, Berkeley, CA, Tech. Rep., 2007.
- [14] R. Vidal and Y. Ma, "A unified algebraic approach to 2-D and 3-D motion segmentation and estimation," *J. Math. Imag. Vision*, vol. 25, no. 3, pp. 403–421, Oct. 2006.
- [15] M. Mishali and Y. C. Eldar, "Blind multiband signal reconstruction: Compressed sensing for analog signals," *IEEE Trans. Signal Process.*, vol. 57, no. 3, pp. 993–1009, Mar. 2009.
- [16] M. Mishali and Y. C. Eldar, "From theory to practice: Sub-Nyquist sampling of sparse wideband analog signals," *IEEE J. Sel. Topics Signal Process.*, vol. 4, no. 2, pp. 375–391, Apr. 2010.
- [17] H. J. Landau, "Necessary density conditions for sampling and interpolation of certain entire functions," *Acta Math.*, vol. 117, no. 1, pp. 37–52, 1967.
- [18] F. Parvaresh, H. Vikalo, S. Misra, and B. Hassibi, "Recovering sparse signals using sparse measurement matrices in compressed DNA microarrays," *IEEE J. Sel. Topics Signal Process.*, vol. 2, no. 3, pp. 275–285, Jun. 2008.
- [19] M. Stojnic, F. Parvaresh, and B. Hassibi, "On the reconstruction of block-sparse signals with an optimal number of measurements," *IEEE Trans. Signal Process.*, vol. 57, no. 8, pp. 3075–3085, Aug. 2009.
- [20] Y. Eldar and H. Rauhut, "Average case analysis of multichannel sparse recovery using convex relaxation," *IEEE Trans. Inf. Theory*, vol. 56, no. 1, pp. 505–519, Jan. 2010.
- [21] F. Bach, "Consistency of the group lasso and multiple kernel learning," *J. Mach. Learn. Res.*, vol. 9, pp. 1179–1225, 2008.
- [22] M. Yuan and Y. Lin, "Model selection and estimation in regression with grouped variables," *J. Royal Statist. Soc.: Ser. B (Statist. Methodol.)*, vol. 68, no. 1, pp. 49–67, 2006.
- [23] J. Huang and T. Zhang, "The benefit of group sparsity," *Ann. Statist.*, vol. 38, no. 4, pp. 1978–2004, 2010.
- [24] Y. C. Eldar, P. Kuppinger, and H. Bölcskei, "Block-sparse signals: Uncertainty relations and efficient recovery," *IEEE Trans. Signal Process.*, vol. 58, no. 6, pp. 3042–3054, Apr. 2010.
- [25] Y. C. Eldar and H. Bölcskei, "Block-sparsity: Coherence and efficient recovery," in *Proc. IEEE Int. Conf. Acoust., Speech, Signal Process.*, 2009, pp. 2885–2888.
- [26] M. Figueiredo, J. Bioucas-Dias, and R. Nowak, "Majorization-minimization algorithms for wavelet-based image restoration," *IEEE Trans. Image Process.*, vol. 16, no. 12, pp. 2980–2991, Dec. 2007.
- [27] K. Rosenblum, L. Zelnik-Manor, and Y. C. Eldar, "Dictionary optimization for block-sparse representations," *IEEE Trans. Signal Process.*, 2010, submitted for publication.



**Lihi Zelnik-Manor** (M'08) received the B.Sc. degree in mechanical engineering from the Technion-Israel Institute of Technology, Haifa, in 1995, where she graduated *summa cum laude*, and the M.Sc. degree (with honors) and the Ph.D. degrees in computer science from the Weizmann Institute of Science in 1998 and 2004, respectively.

After graduating, she was a Postdoctoral Fellow with the Department of Engineering and Applied Science, California Institute of Technology (Caltech), Pasadena. Since 2007, she has been a senior lecturer with the Electrical Engineering Department, Technion. Her research focuses on the analysis of dynamic visual data, including video analysis, and visualizations of multiview data.

Dr. Zelnik-Manor's awards and honors include the Israeli high-education planning and budgeting committee (Vatat) three-year scholarship for outstanding Ph.D. degree students, and the Sloan-Swartz postdoctoral fellowship. She also received the Best Student Paper Award at the IEEE Shape Modeling International Conference 2005 and the AIM@SHAPE Best Paper Award 2005.



**Kevin Rosenblum** received the B.Sc. degree in electrical engineering and the B.A. degree in physics in 2008, and the M.Sc. degree in electrical engineering in 2011 from the Technion-Israel Institute of Technology, Haifa.

He is currently an algorithm engineer with Mobileye's Vehicle Detection division, Jerusalem, and is pursuing the M.B.A. degree at the Tel-Aviv University, Tel-Aviv, Israel. His main areas of interests include signal processing algorithms, image processing, and computer vision.



**Yonina C. Eldar** (S'98–M'02–SM'07) received the B.Sc. degree in physics and the B.Sc. degree in electrical engineering both from Tel-Aviv University (TAU), Tel-Aviv, Israel, in 1995 and 1996, respectively, and the Ph.D. degree in electrical engineering and computer science from the Massachusetts Institute of Technology (MIT), Cambridge, in 2002.

From January 2002 to July 2002, she was a Postdoctoral Fellow with the Digital Signal Processing Group, Massachusetts Institute of Technology (MIT), Cambridge. She is currently a Professor with the Department of Electrical Engineering, Technion—Israel Institute of Technology, Haifa. She is also a Research Affiliate with the Research Laboratory of Electronics, MIT, and a Visiting Professor with Stanford University, Stanford, CA.

Her research interests are in the broad areas of statistical signal processing, sampling theory and compressed sensing, optimization methods, and their applications to biology and optics.

Dr. Eldar was in the Program for Outstanding Students at TAU from 1992 to 1996. In 1998, she held the Rosenblith Fellowship for study in electrical engineering at MIT, and in 2000, she held an IBM Research Fellowship. From 2002 to 2005, she was a Horev Fellow of the Leaders in Science and Technology program at the Technion and an Alon Fellow. In 2004, she was awarded the Wolf Foundation Krill Prize for Excellence in Scientific Research, in 2005 the Andre and Bella Meyer Lectureship, in 2007 the Henry Taub Prize for Excellence in Research, in 2008 the Hershel Rich Innovation Award, the Award for Women with Distinguished Contributions, the Muriel and David Jacknow Award for Excellence in Teaching, and the Technion Outstanding Lecture Award, in 2009 the Technion's Award for Excellence in Teaching, and in 2010 the Michael Bruno Memorial Award from the Rothschild Foundation. She is a member of the IEEE Signal Processing Theory and Methods technical committee and the Bio Imaging Signal Processing technical committee, an Associate Editor for the IEEE TRANSACTIONS ON SIGNAL PROCESSING, the EURASIP *Journal of Signal Processing*, the SIAM *Journal on Matrix Analysis and Applications*, and the SIAM *Journal on Imaging Sciences*, and on the Editorial Board of *Foundations and Trends in Signal Processing*.